

# Free-form reinforced concrete, prestressed concrete, and composite components: Calculation of cross-section values

Florian Zimmert  | Thomas Braml

Department of Civil Engineering and Environmental Sciences, Institute for Structural Engineering, University of the Bundeswehr Munich, Neubiberg, Germany

## Correspondence

Florian Zimmert, Department of Civil Engineering and Environmental Sciences, Institute for Structural Engineering, University of the Bundeswehr Munich, Werner-Heisenberg-Weg 39, 85577 Neubiberg, Germany.  
 Email: [florian.zimmert@unibw.de](mailto:florian.zimmert@unibw.de)

## Funding information

dtec.bw—Digitalization and Technology Research Center of the Bundeswehr; European Union—NextGenerationEU

## Abstract

A resource-efficient use of concrete as a construction material can be achieved by adapting the individual shape of a component under consideration to the stresses that occur and by arranging composite construction materials (e.g., reinforcing steel, prestressing steel, or structural steel) in suitable areas of the component. Due to the advancing digitalization in the construction industry, for example in the context of Building Information Modeling, computer-aided 3D modeling methods are increasingly being used in the planning of structures. These allow engineers to design components in free form. In reinforced concrete, prestressed concrete, and composite construction, the design of such components is currently still associated with great effort. In the context of the development of a practical method for the calculation of free-form concrete components, this paper presents a CAD-integrated method for the calculation of cross-section values. Cross-section values are required as an essential calculation basis when real, three-dimensional structural components are treated using simplified calculation theories, such as the beam theory. In this paper, the mathematical and numerical fundamentals of a method for the calculation of cross-section values of free-form concrete, reinforced concrete, prestressed concrete, and compound components are presented. The calculation method is based on flat geometric regions described by Non-uniform Rational B-Spline tensor product surfaces, which can be extracted from solid models, for example.

## KEYWORDS

B-Splines, composite structures, cross-section values, digitalization, IGA, moments of area, NURBS, prestressed concrete, structural concrete, surfaces, warping torsion

## JEL CLASSIFICATION

C63

## 1 | INTRODUCTION

Due to the advancing digitalization in the construction industry, methods of 3D geometric modeling can be increasingly applied in the

planning of structures. One example is the creation of three-dimensional digital images of structures in the context of Building Information Modeling.<sup>1</sup> For the mathematical description of the component geometry, free-form modeling methods using Non-uniform Rational B-Splines

This is an open access article under the terms of the [Creative Commons Attribution](https://creativecommons.org/licenses/by/4.0/) License, which permits use, distribution and reproduction in any medium, provided the original work is properly cited.

© 2023 The Authors. Published by Ernst & Sohn GmbH.

(NURBS) can be applied.<sup>1-5</sup> These offer the designer the possibility to design reinforced concrete, prestressed concrete, and composite components geometrically freely, to dimension them according to the component loads, and to use construction materials in a resource-efficient way.<sup>1,6-9</sup> However, these advantages are currently in opposition to an increased effort for the calculation and dimensioning of these components. The necessary creation of structural analysis models as beam, bar, or shell structures must be carried out manually for each design step or after each geometric adjustment of the component.<sup>10</sup> A new method is currently investigated that will allow the automated derivation of analysis models from NURBS solid models of (reinforced) concrete members.<sup>11,12</sup> Using the example of a reinforced concrete beam in free form, the main steps of this procedure are shown in Figure 1. In the first step, cross-sections are automatically extracted as planar NURBS surfaces at the points of the NURBS solid model relevant for model generation. Afterwards, cross-section values of these extracted surfaces that are relevant for model formation are calculated and passed on to an algorithm for generating the analysis model. This is then used for the calculation and design of the component at cross-section level and, in a final step, is to generate digital images of reinforcement cages. The continuous use of NURBS solid models with integrated analysis models ensures a complete availability of the digital image of the component—from planning to production. In this paper, the necessary procedure for the calculation of cross-section values based on planar NURBS surfaces is presented.<sup>13</sup>

In Section 2 of this paper, the state of science and technology in computational calculation of cross-section values is summarized. Thereafter, the basics of the free-form description of plane surfaces by means of NURBS (Section 3) as well as the calculation of essential cross-section values (Section 4) are presented. In the two following Sections 5 and 6, the calculation results of the method are validated on two examples and presented on another example. Section 7 summarizes the main contents of the paper and provides an outlook on future research objectives.

For the implementation and presentation of the method presented here, the authors developed a software in the programming language Python including common program packages. A publication of the software is planned after completion of the research and development work.

## 2 | STATE OF SCIENCE AND TECHNOLOGY

The fundamentals for a computational calculation of cross-section values of arbitrarily shaped and compound cross-sections were introduced by Fleißner<sup>14</sup> in 1962 and are still used today in calculation programs (e.g., INCA2, Dlubal RSECTION, SOFiSTiK, or InfoCAD). This procedure is based on a linearization of the cross-section boundary (polygons), which is encircled for the integration of the surface values, see Figure 2A).<sup>14</sup> Lauer<sup>15</sup> and Marín<sup>16</sup> extended these mathematical approaches so that moments of area of arbitrary order could be calculated. Witfeld showed in his publication in 1982<sup>17</sup> that the use of periodic cubic splines for the description of the cross-section boundaries and integration of the surface values leads to advantages in modeling and accuracy, see Figure 2B). Niggli worked with an algorithm for dimensional reduction in numerical calculations with three-dimensional finite elements<sup>18</sup> as part of his dissertation. The numerical solution of the Saint-Venant torsion problem using the Finite Element Method (FEM) was presented by Koczyk and Weese,<sup>19</sup> Gruttmann et al.,<sup>20</sup> Høgsberg and Krenk,<sup>21</sup> and Pilkey,<sup>22</sup> among others. A method for calculating the shear center and the torsional constant was introduced hereby. Sapountzakis and Mokos used the boundary element method for the calculation of the torsional characteristics of composite members.<sup>23</sup>

The method presented in this paper has the advantage over the state of the art in that no discretization of the cross-section boundary elements as polygons is required to calculate the cross-section values. The calculation is performed using solely the geometric description of the component cross-section by means of NURBS surfaces.

## 3 | DESCRIPTION OF PLANE SURFACES USING NURBS

### 3.1 | General

Today, the application of NURBS is considered an industry standard in the field of computer graphics. It enables the efficient modeling of spatial curves, surfaces, and solids, both in free form and for

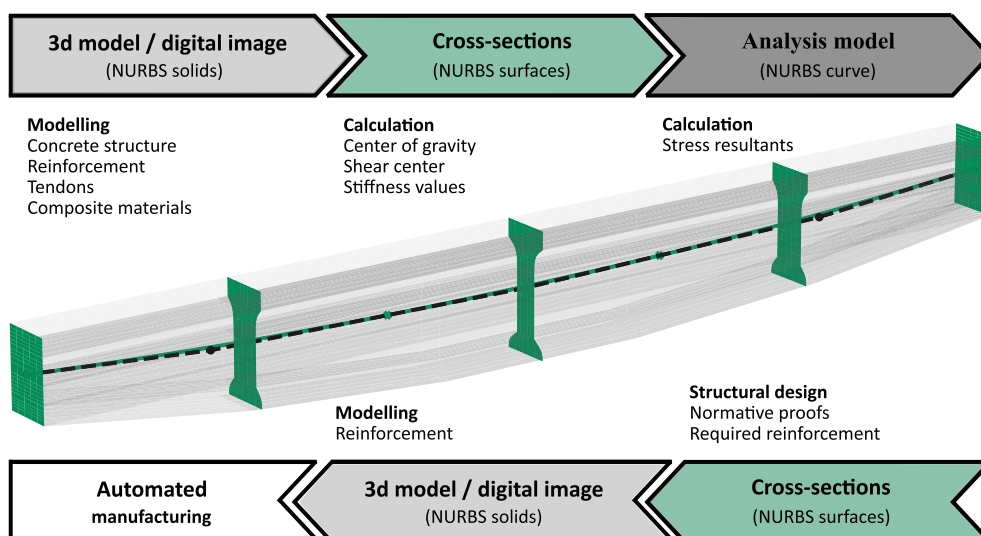


**FIGURE 1** Development of a method for the automated derivation of structural analysis models for free-form structural concrete, prestressed concrete, and compound components in the context of a continuously digital process chain for design and production.

**FIGURE 2** Geometric description of flat regions for the calculation of cross-section values: (A) using polygonal boundaries<sup>14</sup>, (B) using cubic splines.<sup>17</sup>

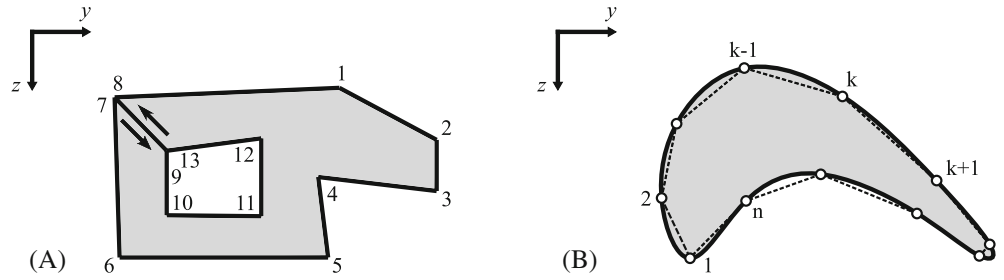


**TABLE 1** Parameters and variables for the definition of NURBS surfaces.

Parameter/variable	Description
$x, y, z$	Cartesian coordinates
<b>P</b>	NURBS control net
$w$	Weight of a NURBS control point
<b>S</b>	NURBS surface
$\xi, \eta$	Parameters for the definition of a surface
$\Xi, H$	Knot vectors
$p, q$	Polynomial degree of the NURBS basis functions
$n, m$	Number of the NURBS basis functions
$i, j, k, l$	Control variables
$N, M$	B-Spline basis functions
$R$	NURBS basis function

Abbreviation: NURBS, Non-uniform Rational B-Splines.

standard analytical shapes (e.g., rectangles, circles), as well as the consistent exchange of geometric data. Geometrically complex objects can be composed of partial objects (patches).<sup>4</sup> NURBS are a generalization of so-called Bézier Splines (B-Splines) and belong to the category of approximating methods for the mathematical description of geometric objects.<sup>5</sup> In contrast to B-Splines, NURBS also allow the description of rational functions. This is necessary, for example, for the modeling of circles or cylinders.<sup>4</sup> NURBS offer significant advantages for modeling geometric objects in free form, such as comprehensive possibilities for (local) geometric adjustment.<sup>4,5</sup> In particular, the properties of the NURBS basis functions should be emphasized, which allow the use of arbitrary continuous functions and the simple computation of local derivatives. These properties are also increasingly used in Isogeometric Analysis (IGA).<sup>24</sup> In the subsequent sections, the fundamentals of surface modeling using NURBS are summarized. In Table 1, relevant parameters and variables are introduced. For a comprehensive description of surface modeling using NURBS, the reader is referred to Cohen et al.<sup>2</sup> and Piegl and Tiller.<sup>4</sup>

### 3.2 | NURBS surfaces

General, spatial surfaces are defined by the double tensor product according to Equation (1) when using NURBS. For this purpose, a

two-dimensional parameter space enclosing the geometry is first introduced with parameters  $\xi$  and  $\eta$  (see Figure 3A). B-Spline basis functions  $N$  and  $M$  of number  $n$  and  $m$  and of degree  $p$  and  $q$  are spanned over this parameter space (see Figure 3B,C), converted into NURBS basis functions (see Section 3.3), and multiplied by previously defined control points **P**. See the black markings in Figure 3D). Using Equation (1), any point  $s \in \mathbb{R}^3$  of the surface can be calculated in the Cartesian coordinate system given a pair of parameters  $\xi$  and  $\eta$ .<sup>4</sup> By an example, this procedure is shown in Figure 3 (star symbols) for  $\xi = 0,25$  and  $\eta = 0,75$ . Using Equations (2) and (3), the two partial first derivatives of the surface can be calculated using the first derivatives of the NURBS basis functions.<sup>4,24</sup> The determinant of the Jacobian matrix is calculated using Equation (4).<sup>25</sup>

$$\mathbf{S}(\xi, \eta) = \sum_{i=1}^n \sum_{j=1}^m R_{i,j,p,q}(\xi, \eta) \mathbf{P}_{ij} \quad (1)$$

$$\frac{d}{d\xi} \mathbf{S}(\xi, \eta) = \sum_{i=1}^n \sum_{j=1}^m \frac{d}{d\xi} R_{i,j,p,q}(\xi, \eta) \mathbf{P}_{ij} \quad (2)$$

$$\frac{d}{d\eta} \mathbf{S}(\xi, \eta) = \sum_{i=1}^n \sum_{j=1}^m \frac{d}{d\eta} R_{i,j,p,q}(\xi, \eta) \mathbf{P}_{ij} \quad (3)$$

$$\det(\mathbf{J}) = \left| \frac{d}{d\xi} \mathbf{S}(\xi, \eta) \times \frac{d}{d\eta} \mathbf{S}(\xi, \eta) \right| \quad (4)$$

### 3.3 | Control points, NURBS basis functions, and knot vectors

As input parameters of a NURBS surface description according to Equations (1)–(3), a net of control points  $\mathbf{P}_{ij} \in \mathbb{R}^3$  in the Cartesian (physical) coordinate system as well as a polynomial degree  $p$  and  $q$  for both parameter directions  $\xi$  and  $\eta$  must be specified. The number of required control points is then  $n \geq (p+1)$  and  $m \geq (q+1)$ . Each control point must also be assigned a “weight”  $w_{ij} \in \mathbb{R}$ . To generate the NURBS basis functions according to Equations (6)–(8), two knot vectors  $\Xi$  and  $H$  are to be defined according to Equations (5).<sup>3,4</sup> The parameter values therein always have to be defined in ascending order and usually start at 0 and end at 1. Further information on the calculation of partial derivatives of NURBS basis functions can be found, for example, in Piegl and Tiller<sup>4</sup> or Cottrell et al.<sup>24</sup>

$$\Xi = \left\{ \underbrace{0, \dots, 0}_{p+1}, \xi_{p+1}, \dots, \xi_{n-p-1}, \underbrace{1, \dots, 1}_{p+1} \right\} \quad (5)$$

(analogously valid for  $H$  with  $q$  instead of  $p$  and  $m$  instead of  $n$ )

$$N_{i,0}(\xi) = \begin{cases} 1, & \text{if } \xi \in [\xi_i, \xi_{i+1}[ \\ 0, & \text{otherwise.} \end{cases} \quad (6)$$

$$N_{i,p}(\xi) = \frac{\xi - \xi_i}{\xi_{i+p} - \xi_i} \cdot N_{i,p-1}(\xi) + \frac{\xi_{i+p+1} - \xi}{\xi_{i+p+1} - \xi_{i+1}} \cdot N_{i+1,p-1}(\xi) \quad (7)$$

(analogously valid for  $M$  with  $\eta$  instead of  $\xi$ ,  $q$  instead of  $p$  and  $m$  instead of  $n$ )

$$R_{ij,p,q}(\xi, \eta) = \frac{N_{i,p}(\xi) M_{j,q}(\eta) w_{ij}}{\sum_{i=1}^n \sum_{j=1}^m \sum_{k=1}^n \sum_{l=1}^m N_{k,p}(\xi) M_{l,q}(\eta) w_{k,l}} \quad (8)$$

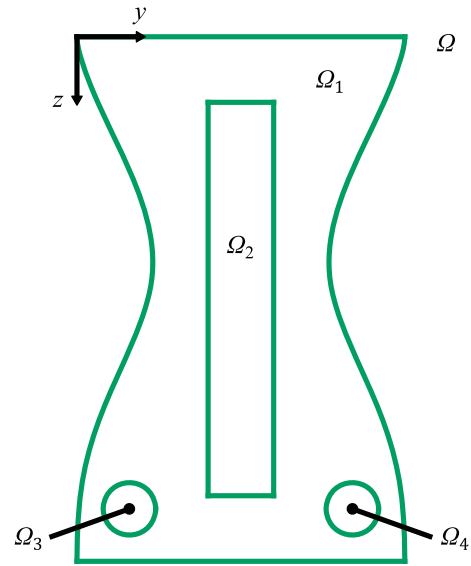


**FIGURE 4** Flat geometric region  $\Omega$  composed of subregions  $\Omega_a$  with local coordinate system.

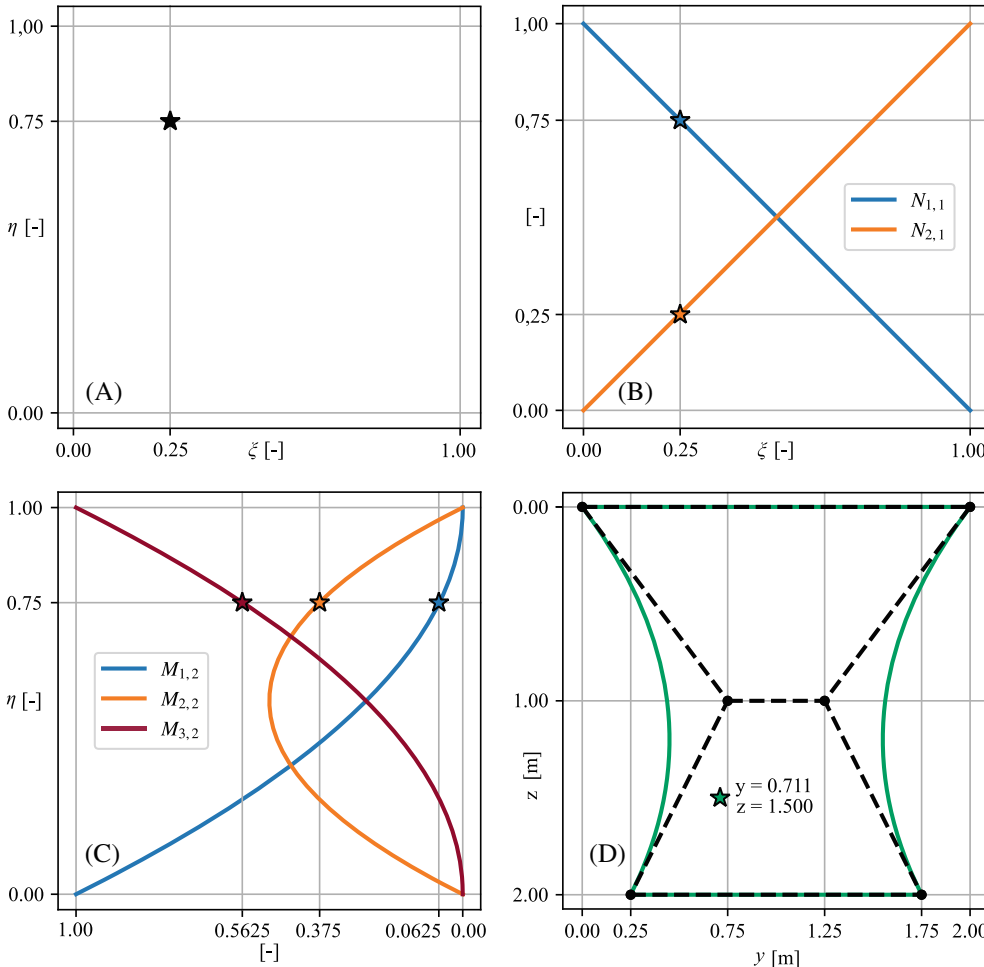


**FIGURE 3** Representation of a NURBS surface with  $p = 1$  and  $q = 2$ . (A) Parameter space; (B) NURBS basis functions for  $\xi$ ; (C) NURBS basis functions for  $\eta$ ; and (D) Physical space with geometry of the surface.

## 4 | CHARACTERISTIC VALUES OF ARBITRARILY SHAPED CROSS-SECTIONS

### 4.1 | Definitions

For the description of cross-sections and cross-section parts, a local, two-dimensional, Cartesian coordinate system is introduced, whose  $y$ -axis points to the right and whose  $z$ -axis points downwards, see Figure 4. In the context of this paper, only flat surfaces are treated ( $x = 0$ ). The geometric area of the total cross-section is denoted by  $\Omega$ , that of partial cross-sections is denoted by  $\Omega_a$  for  $a \in [1, n_a]$ , where  $n_a$  reflects the maximum number of partial cross-sections.<sup>17</sup> Each of these partial cross-sections may be assigned a different material. When describing partial sections  $\Omega_a$  according to Figure 4,  $\Omega_{a,c} :=$  concrete,  $\Omega_{a,s} :=$  reinforcement,  $\Omega_{a,p} :=$  prestressing steel,  $\Omega_{a,d} :=$  duct,  $\Omega_{a,h} :=$  hole or  $\Omega_{a,cp} :=$  composite material is valid.

For the cross-section values considered, the formula symbols and units according to Table 2 apply. The notation for the static moments ( $S_y$  or  $S_z$ ) and for the area moments of inertia and the product of inertia ( $I_y, I_z$  and  $I_{yz}$ ) are replaced by area moments of higher degree following<sup>15</sup> for reasons of easier distinguishability.

In the following, the mathematical and numerical fundamentals for the calculation of the cross-sectional values of arbitrarily shaped and composite surfaces (by means of NURBS) are summarized, taking into account the definitions already presented. These are based on the Gauss's theorem for the plane surface and the numerical solution of the Saint-Venant torsion problem and are independent of the selected position of the cross-section in the reference coordinate system.<sup>14,17,26</sup> Characteristic values, which are marked with a tilde, refer to the origin of the preselected, local coordinate system and must be transformed afterwards to the center of gravity of the total cross-section.

### 4.2 | Gross, net, and ideal cross-section values

When calculating cross-section values of reinforced concrete, prestressed concrete, and composite components, a distinction is made

between gross, net, and ideal cross-section values in the cases listed below, see Table 3.<sup>26</sup> Gross cross-section values describe the entire structural member without taking into account included reinforcing steel, prestressing steel, or ungrouted ducts. When calculating net cross-section values, ungrouted ducts are subtracted (pretension with subsequent bond). Ideal cross-section values take into account the different material properties of concrete, reinforcing steel, prestressing steel as well as other existing composite construction materials such as steel or wood.<sup>26</sup> For the calculation of ideal cross-section values, a reference value of elastic deformation properties (Young's modulus or G-modulus)  $\alpha_{a,ref}$  and  $\beta_{a,ref}$  must be defined for each different construction material (index  $a$ ) according to Equations (9) and (10).<sup>22</sup> Usually, the Young's modulus and the G-modulus of the dominant construction material are used as reference values.<sup>22</sup> Rigid bond between different construction materials is assumed for the cross-section.

**TABLE 3** Distinction between gross, net, and ideal cross-section values and their respective usage.

Notation	Application
Gross (Index, g)	<ul style="list-style-type: none"> <li>General reinforced concrete components.</li> <li>Prestressed concrete components (for design purposes).</li> </ul>
Net (Index, n)	<ul style="list-style-type: none"> <li>Prestressed concrete components during states of construction with ungrouted ducts (prestressing with subsequent bond).</li> </ul>
Ideal (Index, i)	<ul style="list-style-type: none"> <li>Reinforced concrete components with high accuracy requirements (e.g. for deformation calculations).</li> <li>Prestressed concrete components (prestressing with instant bond).</li> <li>Prestressed concrete components with grouted ducts (prestressing with subsequent bond).</li> <li>Composite components.</li> </ul>

**TABLE 2** Definition of the general cross-section values in the local coordinate system according to Figure 4.

Description	Notation	Unit
Moment of area of arbitrary order	$A_{y^i z^j}$	$(m^{2+\max(i,j)})$
Zerth moment of area (area)	$A$	$(m^2)$
First moments of area (static moments)	$A_y$ $A_z$	$(m^3)$
Second moments of area (area moments of inertia)	$A_{yy}$ $A_{yz}$ $A_{zz}$	$(m^4)$
Third moments of area	$A_{yyy}$ $A_{yyz}$ $A_{yzz}$ $A_{zzz}$	$(m^5)$
Coordinates of the center of gravity	$s_y$ $s_z$	$(m)$
Principal bending angle	$\varphi_0$	$(^\circ)$
Principal moments of inertia	$A_{\xi\xi}$ $A_{\eta\eta}$	$(m^4)$
Torsional constant	$A_{xx}$	$(m^4)$
Coordinates of the shear center	$s_{my}$ $s_{mz}$	$(m)$

$$\alpha_{a,\text{ref}} = \frac{E_a}{E_{\text{ref}}} \quad (9)$$

$$\beta_{a,\text{ref}} = \frac{G_a}{G_{\text{ref}}} \quad (10)$$

When calculating cross-section values of reinforced concrete, prestressed concrete, and composite structures, a distinction must also be made between the uncracked state (“State I”) and the cracked state (“State II”).<sup>26</sup> The calculation method presented here is applicable to both cases.<sup>15</sup>

### 4.3 | Moments of area

The moments of area of degree  $\chi, \psi$  are calculated for the total cross-section according to Equation (11).<sup>14–17</sup> Generally, these are the moments of area of zeroth to third degree already listed in Table 2. Third-degree moments of area are not directly required for linear-elastic calculations of internal forces, strains, or stresses and are therefore often not well-known. However, they are used for the integration of non-linearly distributed cross-sectional stresses. These can occur, for example, in the compression zone of reinforced concrete members subjected to bending loads and serve as input variables for the iterative determination of the force equilibrium at the cracked cross-section.<sup>15</sup> For cross-section components  $\Omega_{a,d}$  (duct) and  $\Omega_{a,h}$  (hole), a negative sign is to be placed in front of the integral in Equation (11).

$$\tilde{A}_{\chi\psi} = \sum_{a=1}^{n_a} \alpha_{a,\text{ref}} \iint_{\Omega_a} y^\chi z^\psi d\Omega_a \quad (11)$$

### 4.4 | Location of the center of gravity

The location of the center of gravity of the total cross section with respect to the origin of the chosen local coordinate system, is calculated according to Equations (12) and (13).<sup>14–17</sup>

$$s_y = \frac{\tilde{A}_y}{A} \quad (12)$$

$$s_z = \frac{\tilde{A}_z}{A} \quad (13)$$

### 4.5 | Center of gravity transformation

If the coordinates of the calculated center of gravity  $s_y$  and  $s_z$  do not coincide with the origin of the chosen local coordinate system, a transformation of the cross-section values according to Equation (14) is required.<sup>14–17</sup>

$$A_{\chi\psi} = \tilde{A}_{\chi\psi} - A \cdot s_y^\chi \cdot s_z^\psi \quad (14)$$

### 4.6 | Principal bending angle and principal moments of inertia

If a product of inertia is existent ( $A_{yz} \neq 0$ ), the principal moments of inertia  $A_{\xi\xi}$  and  $A_{\eta\eta}$  differ from the area moments of inertia  $A_{yy}$  and  $A_{zz}$  in their direction of action and magnitude. The principal bending angle and the corresponding principal moments of inertia are calculated by Equations (15)–(17).<sup>14–17</sup>

$$\tan(2\varphi_0) = \frac{2 \cdot A_{yz}}{A_{yy} - A_{zz}} \quad (15)$$

$$A_{\xi\xi} = \frac{A_{yy} + A_{zz}}{2} + \left[ \frac{A_{yy} - A_{zz}}{2} \cdot \cos(2\varphi_0) - A_{yz} \cdot \sin(2\varphi_0) \right] \quad (16)$$

$$A_{\eta\eta} = \frac{A_{yy} + A_{zz}}{2} - \left[ \frac{A_{yy} - A_{zz}}{2} \cdot \cos(2\varphi_0) - A_{yz} \cdot \sin(2\varphi_0) \right] \quad (17)$$

### 4.7 | Warping function

The calculation of the torsional constant  $A_{xx}$  as well as the location of the shear center  $s_{my}$  and  $s_{mz}$  of arbitrarily shaped cross-sectional areas requires the solution of Laplace's equation (Saint-Venant torsion) of the warping function  $\omega$  according to Equation (18), respecting the condition for the boundary of the cross-section given by Equation (19).<sup>19,20,22</sup> In the following, the basic steps for the numerical calculation of the warping function  $\omega$  by means of IGA, that is, using the NURBS basis functions, are presented.

First, analogous to the “classical” FEM, a weak form of the boundary value problem is described according to Equations (18) and (19) using the calculus of variations. The test and weighting functions generated in this process have the NURBS basis functions of the geometric description as their basis and are partitioned into finite subsets (elements) of the entire solution space (Bubnov–Galerkin method).<sup>24,25</sup> The element-wise approximation of the sought warping function is then described by Equation (20). Analogous to the “classical” FEM, stiffness matrices and load vectors can now be generated for each element. These are given in Equations (21) and (22) for the numerical calculation of the warping function.<sup>22</sup> After the assembly of the global stiffness matrix and the global load vector from the element-wise contributions, the linear system of equations, see Equation (23), can be solved and the discrete values of the warping function can be determined.<sup>24</sup> For this purpose, an arbitrary degree of freedom has to be provided with a restraint (Dirichlet boundary condition).<sup>19</sup> Also in IGA, adequate refinement of the calculation is essential for the accuracy of the result. For this purpose, methods for increasing the degree of the basis functions (p-method) as well as for mesh refinement of the surface (h-method) are available. These can also be used in combination (hp-method).<sup>24</sup> The definition of elements in the context of IGA is given in Section 4.9. Further theoretical background and practical hints for the implementation



and application of IGA can be found, for example, in Cottrell et al.<sup>24</sup> and Hughes.<sup>25</sup>

$$\Delta\omega = \nabla^2\omega = \frac{\partial^2\omega}{\partial y^2} + \frac{\partial^2\omega}{\partial z^2} = 0 \quad (\text{in } \Omega) \quad (18)$$

$$\left(\frac{\partial\omega}{\partial y} - z\right)n_y + \left(\frac{\partial\omega}{\partial z} + y\right)n_z = 0 \quad (\text{at the boundary of } \partial\Omega) \quad (19)$$

with  $\mathbf{n}$  defined as the unit normal vector of the cross-section boundary.

$$\omega_e^a(\xi, \eta) = \sum_{i=1}^{n_a^e} \sum_{j=1}^{m_a^e} R_{ij,p,q,a}^e(\xi, \eta) \omega_{ij,a}^e = \mathbf{R}_a^e(\xi, \eta) \boldsymbol{\omega}_a^e \quad (20)$$

$$\mathbf{k}_a^e = \beta_{a,\text{ref}} \cdot \iint_{\Omega_e^a} \left( \frac{\partial \mathbf{R}^T}{\partial y} \frac{\partial \mathbf{R}}{\partial y} + \frac{\partial \mathbf{R}^T}{\partial z} \frac{\partial \mathbf{R}}{\partial z} \right) d\Omega_e^a \quad (21)$$

$$\mathbf{p}^e = \beta_{a,\text{ref}} \cdot \iint_{\Omega_e^a} \left( \frac{\partial \mathbf{R}}{\partial z} \cdot y - \frac{\partial \mathbf{R}}{\partial y} \cdot z \right) d\Omega_e^a \quad (22)$$

$$\mathbf{K}\boldsymbol{\omega} = \mathbf{P} \quad (23)$$

## 4.8 | Shear center and torsional constant

The result of the numerical calculation are discrete values of the basic warping function  $\omega$ , which are converted into values of an adjusted unit warping function  $\bar{\omega}$  by Equation (24). Using this, the coordinates of the shear center (with respect to the coordinate origin) can be calculated according to Equations (25)–(28). Subsequently the values of the principal warping function  $\tilde{\omega}$  can be calculated by means of Equation (29). The torsional constant is calculated via the principal warping function according to Equation (30).<sup>19,20,22</sup>

$$\bar{\omega} = \omega - \frac{1}{A} \sum_{a=1}^{n_a} \beta_{a,\text{ref}} \sum_{e=1}^{n_{e,a}} \iint_{\Omega_e^a} \omega_e^a d\Omega_e^a \quad (24)$$

$$A_{\bar{\omega}y} = \sum_{a=1}^{n_a} \beta_{a,\text{ref}} \sum_{e=1}^{n_{e,a}} \iint_{\Omega_e^a} \bar{\omega}_e^a y d\Omega_e^a \quad (25)$$

$$A_{\bar{\omega}z} = \sum_{a=1}^{n_a} \beta_{a,\text{ref}} \sum_{e=1}^{n_{e,a}} \iint_{\Omega_e^a} \bar{\omega}_e^a z d\Omega_e^a \quad (26)$$

$$S_{my} = \frac{A_{\bar{\omega}y} \cdot A_{yz} - A_{\bar{\omega}z} \cdot A_{yy}}{A_{yy} \cdot A_{zz} - A_{yz}^2} \quad (27)$$

$$S_{mz} = \frac{A_{\bar{\omega}y} \cdot A_{zz} - A_{\bar{\omega}z} \cdot A_{yz}}{A_{yy} \cdot A_{zz} - A_{yz}^2} \quad (28)$$

$$\tilde{\omega} = \bar{\omega} + S_{my} \cdot z - S_{mz} \cdot y \quad (29)$$

$$A_{xx} = A_{zz} + A_{yy} - \bar{\boldsymbol{\omega}}^T \mathbf{K}\boldsymbol{\omega} \quad (30)$$

## 4.9 | Numerical integration

The integrals appearing in Equations (11), (21), (22), and (24)–(26) for the calculation of the cross-section values can be calculated within numerical accuracy using Gauss quadrature.<sup>25</sup> This is also true in the case where NURBS basis functions are used for geometric description.<sup>4,24</sup> For this purpose, first the two knot vectors  $\Xi$  and  $H$ , which describe the NURBS basis functions of the respective cross-section parts, must be subdivided into elements  $E_{n_e}$  (number:  $n_e$ ) with the spans  $[\xi_i, \xi_{i+1}]$  and  $[\eta_i, \eta_{i+1}]$ . Note that  $\xi_{i+1} > \xi_i$  and  $\eta_{i+1} > \eta_i$ .<sup>24</sup> This step is exemplified in Equations (31) and (32), respectively. Within the parameter intervals of each element defined in this way,  $n_{\text{gp},\xi} = (p+1)$  and  $n_{\text{gp},\eta} = (q+1)$  Gaussian points are defined. Thus, the number of required Gaussian points depends on the degree of the chosen basis functions for the geometric description and is  $n_{\text{gp}} = n_{\text{gp},\xi} \cdot n_{\text{gp},\eta}$ . The number of Gaussian points determines their location in the uniform parameter space  $\tilde{\xi}_{\text{gp}} \in [-1, 1]$  and  $\tilde{\eta}_{\text{gp}} \in [-1, 1]$  as well as their weights  $\alpha_{\text{gp},\xi}$  and  $\alpha_{\text{gp},\eta}$ . A detailed description of how to compute the location of the Gaussian points as well as their associated weights can be found in, for example, Hughes<sup>25</sup> or Stroud and Secrest.<sup>27</sup>  $\tilde{\xi}_{\text{gp}}$  and  $\tilde{\eta}_{\text{gp}}$  must now be transformed to the parameter space of the respective element using Equation (33).<sup>25,27</sup> At these points, the values of the function to be integrated are then calculated and multiplied by associated weights  $\alpha_{\text{gp},\xi}$  and  $\alpha_{\text{gp},\eta}$ , and the determinant of the Jacobian matrix, see Equation (4). Finally these are added to the total value of the respective cross-sectional part, see Equation (34). The use of the Gauss quadrature achieves sufficiently accurate results in the integration of NURBS surfaces for the application presented here.<sup>24</sup> The location and the weights of the Gaussian points for the numerical integration of the surface according to Figure 3 are exemplarily shown in Figure 5.

$$\Xi = \left\{ \begin{array}{c} 0, 0, 0, 5, 1, 1 \\ [E_1 | E_2] \end{array} \right\} \quad (31)$$

$$H = \left\{ \begin{array}{c} 0, 0, 0, 0, 5, 1, 1, 1 \\ [E_1 | E_2] \end{array} \right\} \quad (32)$$

$$\xi_{\text{gp}} = \frac{(\xi_{i+1} - \xi_i)}{2} \cdot \tilde{\xi}_{\text{gp}} + \frac{(\xi_{i+1} + \xi_i)}{2} \quad (33)$$

(Analogously valid for  $\eta_{\text{gp}}$ ).

$$\iint_{\Omega_a} f(x, y) d\Omega_a = \sum_{e_a=1}^{n_{e,a}} \frac{\xi_{i+1} - \xi_i}{2} \sum_1^{n_{\text{gp},e,a}} f(\xi_{\text{gp},e,a}, \eta_{\text{gp},e,a}) \cdot \alpha_{\text{gp},\xi,e,a} \cdot \alpha_{\text{gp},\eta,e,a} \cdot \det(\mathbf{J}) \quad (34)$$

## 5 | VALIDATION OF CALCULATION RESULTS

In the following, the results of the presented method for calculating cross-section values are validated using two examples with available

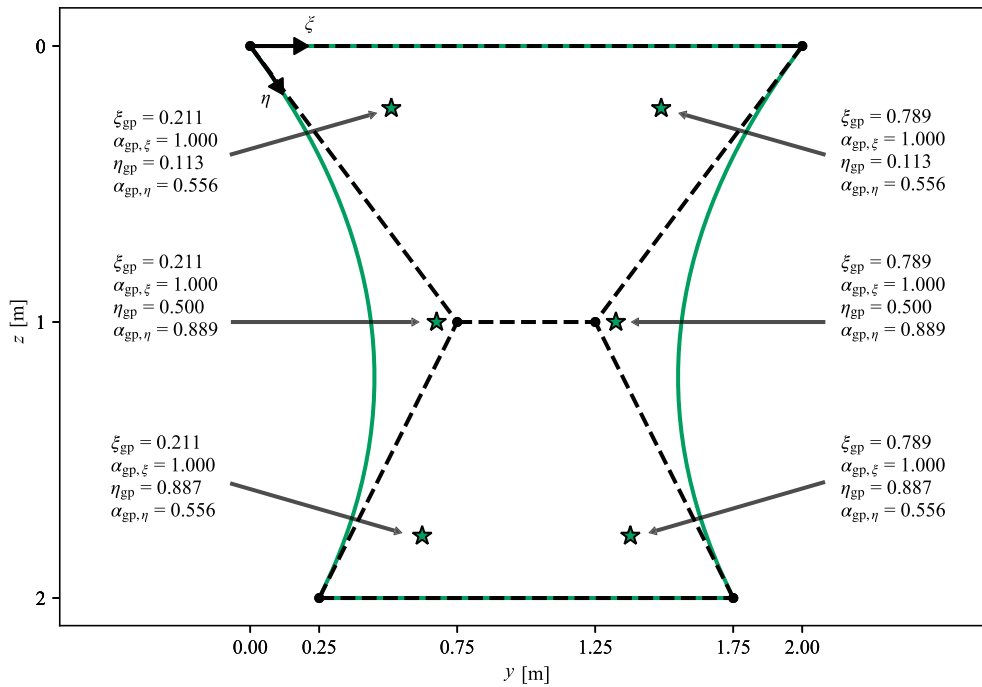


**FIGURE 5** Location and weights of the Gaussian quadrature points (green stars) for the integration of the NURBS surface of Figure 3.

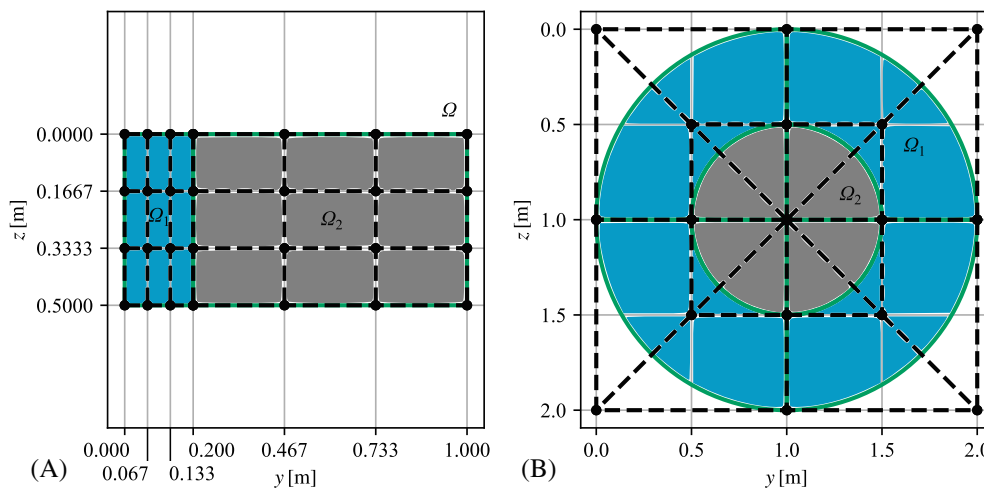


**FIGURE 6** Geometry of the compound cross-sections for the validation of results: (A) rectangular cross-section; (B) circular cross-section.

analytical (approximate) solutions. The composite cross-section  $\Omega$  considered in both cases consists of two partial surfaces  $\Omega_1$  and  $\Omega_2$  with the respective dimensions according to Figure 6. Example 1 describes two connected rectangles with control points according to Figure 6(A) as well as  $p=q=3$  and  $\Xi = H = [0,0,0,1,1,1,1]$  in each case. Example 2 describes two concentrically arranged circles with radii according to Figure 6(B). The modeling of circular surfaces using NURBS is discussed in detail in Piegel and Tiller.<sup>4</sup> In both examples, a concrete of grade C20/25 is assigned to subarea  $\Omega_1$  as the construction material and a concrete of grade C50/60 is assigned to subarea  $\Omega_2$ . With reference to the concrete of grade C50/60, the reference values of the material properties are:  $\alpha_{1,ref} = \beta_{1,ref} = 0,803746$  and  $\alpha_{2,ref} = \beta_{2,ref} = 1,00$ . The analytical solutions for the moments of area and the location of the center of gravity are available in tabular form in the literature, see, for example, Pilkey<sup>28</sup> and are therefore not listed separately here. A formula for the

approximate calculation of the torsional constant is given for Example 1 in Equation (35) and for Example 2 in Equation (36).<sup>22,29</sup> In Table 4, the results of the presented calculation method are compared with the analytical solutions. A very good match of the results can be observed with a maximum difference of 1.6%. This is due to the fact that Equation (36) is an approximate formula.

$$A_{xx,\Omega,1} = \frac{1}{3} (\alpha_{1,ref} \cdot b_{\Omega_1} + b_{\Omega_2}) \cdot h^3 - 3,361 \cdot \frac{h^4}{16} \cdot \frac{1 + \alpha_{1,ref}^2}{1 + \alpha_{1,ref}} \quad (35)$$

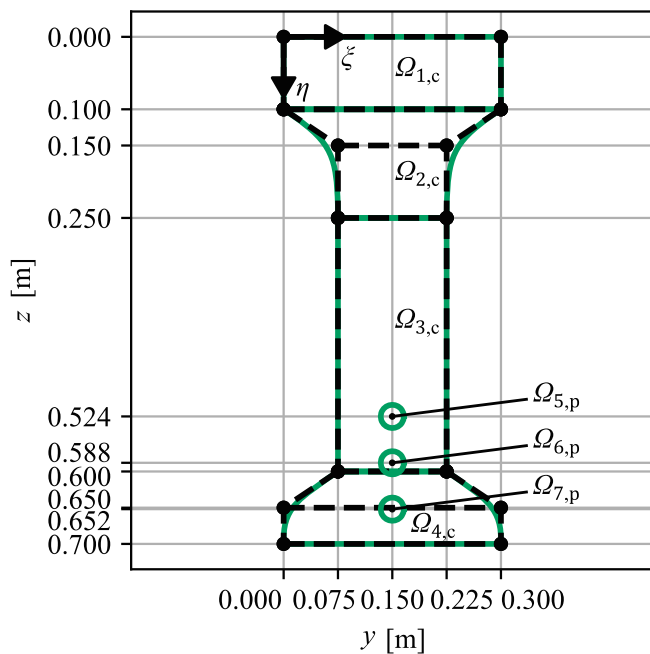
$$A_{xx,\Omega,2} = \left[ 1 + \frac{2 \cdot (\alpha_{1,ref} - 1)}{\alpha_{1,ref} + 1} \cdot \frac{A_{xx,\Omega_2}}{A_{xx,\Omega_0}} \right] \cdot A_{xx,\Omega_0} \quad (36)$$

with  $b_{\Omega_1}, b_{\Omega_2}$  as the width of the respective cross-sectional part;  $h$  as the height of the cross-section; and  $A_{xx,\Omega_0}$  as the torsional constant of a fictitious, homogeneous total cross-section.



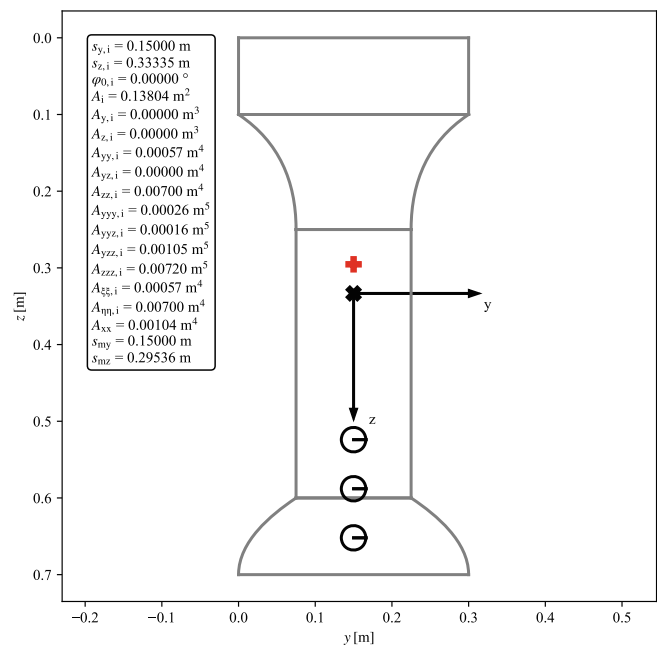
**TABLE 4** Comparison of the numerical and analytical solution for the values of the cross-sections according to Figure 6.

Cross-section value	Numerical solution		Analytical solution		Difference		Unit
	Example 1	Example 2	Example 1	Example 2	Example 1	Example 2	
A	0.480375	2.987731	0.480375	2.987455	0%	< 0.01%	(m <sup>2</sup> )
$A_y = A_z = A_{yz}$	0	0	0	0	0%	0%	(m <sup>3</sup> )
$A_{yy}$	0.038333	0.775836	0.038333	0.775765	0%	< 0.01%	(m <sup>4</sup> )
$A_{zz}$	0.010007	0.775836	0.010007	0.775765	0%	< 0.01%	(m <sup>4</sup> )
$s_y$	0.516342	1.0	0.516342	1.0	0%	0%	(m)
$s_z$	0.25	1.0	0.25	1.0	0%	0%	(m)
$A_{xx}$	0.027607	1.551635	0.028050	1.549433	1.6%	0.14%	(m <sup>4</sup> )
$s_{my}$	0.516342	0.999995	0.516342	1.0	0%	< 0.01%	(m)
$s_{mz}$	0.25	0.999995	0.25	1.0	0%	< 0.01%	(m)

**FIGURE 7** Cross-section at the mid-span of the prestressed girder according to Figure 1; geometry in green; control net in black.

## 6 | EXAMPLE

In the following, the presented calculation method for cross-section values is applied to an example. The characteristic values of the cross-section in the midspan of a prestressed concrete girder are calculated. This girder, already shown in Figure 1, was modeled as a shape-optimized component following Rath et al.<sup>30</sup> The cross-section shown in Figure 7 consists of seven partial surfaces:  $\Omega_{1,c}$ ,  $\Omega_{2,c}$ ,  $\Omega_{3,c}$ , and  $\Omega_{4,c}$  describe the concrete body and  $\Omega_{5,p}$ ,  $\Omega_{6,p}$ ,  $\Omega_{7,p}$  the prestressing steel cross-section with a respective cross-sectional area of  $A_p = 150 \text{ mm}^2$ . The control points for modeling these subareas are given in Figure 7, and the knot vectors and the degrees of the NURBS basis functions are listed below. To avoid clutter, for the tendons, only their location is given in Figure 7. The modeling of circular surfaces

**FIGURE 8** Ideal cross-section values at the mid-span of the prestressed girder according to Figure 1.

using NURBS is described thoroughly in Pieggl and Tiller.<sup>4</sup> The calculated ideal cross-section values are given in Figure 8. In addition, the warping function calculated using IGA is shown qualitatively in Figure 9. For its calculation, the NURBS basis functions of the geometric description were increased to the degree  $p = q = 3$  (p-method). No further mesh refinement was applied.

$$\Xi_{\Omega_{1,c}} = \Xi_{\Omega_{2,c}} = \Xi_{\Omega_{3,c}} = \Xi_{\Omega_{4,c}} = [0, 0, 1, 1]$$

$$H_{\Omega_{1,c}} = H_{\Omega_{3,c}} = [0, 0, 1, 1]; \quad H_{\Omega_{2,c}} = H_{\Omega_{4,c}} = [0, 0, 0, 1, 1, 1]$$

$$p_{\Omega_{1,c}} = p_{\Omega_{2,c}} = p_{\Omega_{3,c}} = p_{\Omega_{4,c}} = 1$$

$$q_{\Omega_{1,c}} = q_{\Omega_{3,c}} = 1; \quad q_{\Omega_{2,c}} = q_{\Omega_{4,c}} = 2.$$

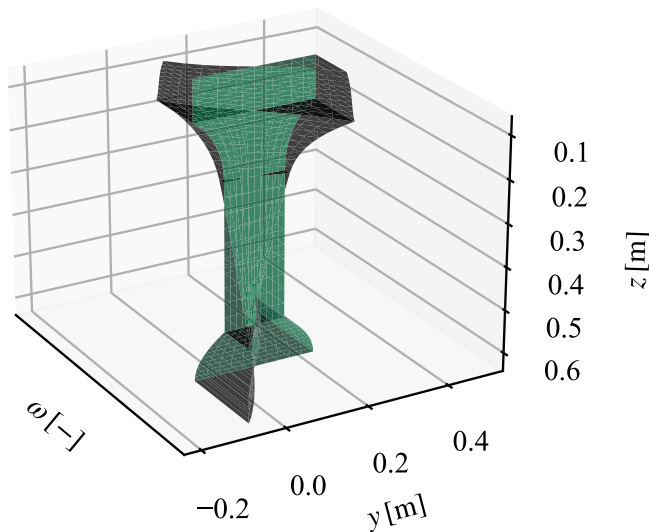


**FIGURE 9** Warping function (qualitative representation) of the cross-section at the mid-span of the prestressed girder according to Figure 1.

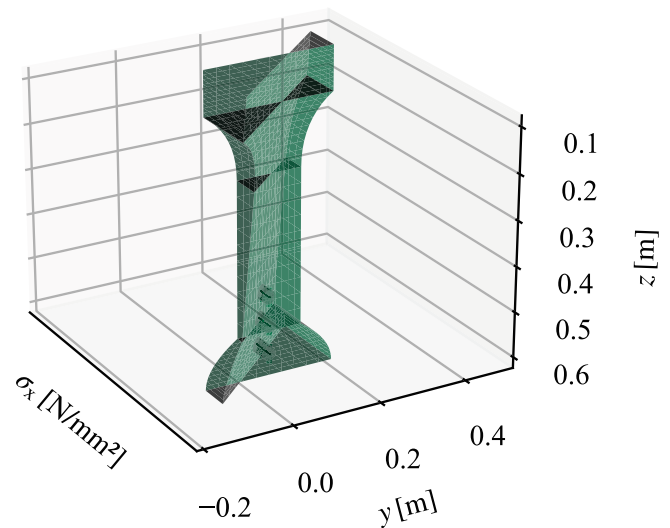


**FIGURE 10** Cross-section stresses (qualitative representation) as result of biaxial bending with longitudinal force at the mid-span of the prestressed beam according to Figure 1.

## 7 | CONCLUSIONS AND OUTLOOK

In this paper, the fundamentals for the calculation of cross-section values of free-form reinforced concrete, prestressed concrete, and composite components are presented. The cross-sections are described by NURBS surfaces. The element-wise integration of the moments of area and other geometric values is easily possible using Gauss quadrature. The calculation of the torsional values is performed by a numerical approximation using IGA. In a further step, convergence studies shall be carried out so that rules for a generally sufficient refinement of this numerical calculation can be determined. The calculation results of the method implemented by the authors in the programming language Python were validated on two examples with analytical solutions. The application was demonstrated on another example. It is expected that due to new manufacturing techniques, such as concrete 3D printing, the description of free forms will play an important role in the future.<sup>12</sup> For the procedure presented in Section 1 for the structural analysis and design of such components, the following further steps are necessary.

- Automatic calculation of the location as well as the geometry of finite elements (bars or beams) from NURBS solids.<sup>11</sup> This can be achieved, for example, by means of an interpolation of previously calculated center of gravity coordinates by NURBS curves, see Figure 1.<sup>4</sup>
- Calculation of stiffness matrices of the generated finite elements using locally calculated cross-section values and preselected construction material properties.<sup>25</sup>
- Generation of load vectors from actions and calculation of deformations using IGA.<sup>24</sup>
- Investigation of the limits of validity of the applied beam theory for different geometric shapes by means of comparison with solid models.

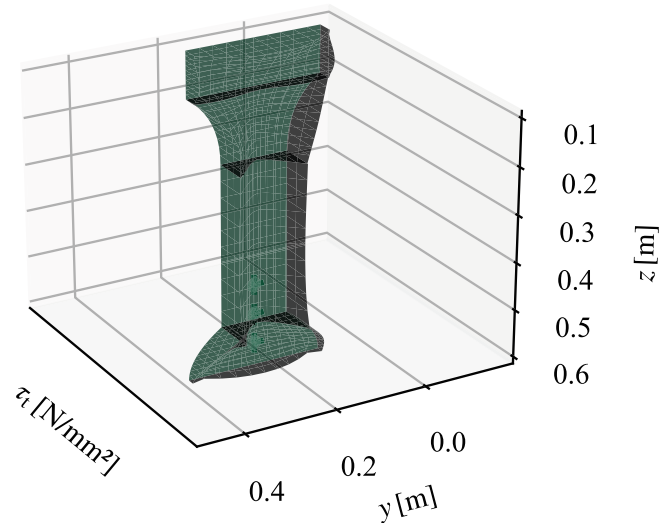


**FIGURE 11** Cross-section stresses (qualitative representation) as result of torsion at the mid-span of the prestressed beam according to Figure 1.

- Calculation of internal forces using IGA.<sup>24</sup>
- Cross-sectional design for biaxial bending with longitudinal force as well as torsion and biaxial shear force loading using cross-sections extracted locally as NURBS surfaces.<sup>15</sup> The calculation of cross-sectional stresses required for this purpose is exemplified in Figure 10 (biaxial bending with longitudinal force) and Figure 11 (torsion).<sup>22</sup>
- Generation of digital images of reinforcement cages as NURBS solids using cross-section-related design results.
- Optimization of structural components with respect to the usage of construction materials.

## AUTHOR CONTRIBUTIONS

**Florian Zimmert:** Conceptualization; methodology; formal analysis; investigation; visualization; writing - original draft preparation and editing. **Thomas Braml:** Supervision; writing - review; funding acquisition.

## ACKNOWLEDGMENTS

This research work has been carried out within the project DEFINE and is funded by dtec.bw—Digitalization and Technology Research Center of the Bundeswehr, which we gratefully acknowledge. dtec.bw is funded by the European Union—NextGenerationEU. Within the project DEFINE, methods of free-form modeling as well as structural-mechanical and building-physical optimization are applied to a novel AC/DC converter station for medium voltage networks. Additional thanks goes to Mr Laines Gerhardt, MSc for his support during the software development in the context of his master's thesis at the UniBw M as well as to the developers of the freely available programming language Python including related program packages.

## DATA AVAILABILITY STATEMENT

The data that support the findings of this study are available from the corresponding author upon reasonable request.

## ORCID

Florian Zimmert  <https://orcid.org/0000-0002-2411-1106>

## REFERENCES

- Borrmann A, König M, Koch C, Beetz J. Building Information Modeling—Technologische Grundlagen und industrielle Praxis. 2nd ed. Wiesbaden: Springer Vieweg Wiesbaden; 2021.
- Cohen E, Riesenfeld RF, Elber G. Geometric Modeling with Splines—An Introduction. Natick, MA: AK Peters; 2001.
- Farin G. Curves and surfaces for CAGD—a practical guide. 5th ed. San Diego: Academic Press Books—Elsevier; 2001.
- Piegl L, Tiller W. The NURBS book. 2nd ed. Berlin, Heidelberg, New York: Springer Verlag; 1997.
- Salomon D. Curves and Surfaces for Computer Graphics. New York: Springer Science+Business Media; 2006.
- Breitenberger M, Wüchner R, Bletzinger K-U. Entwurf und Berechnung von gekrümmten Betonfertigbauteilen mit CAD-basierten Verfahren. Beton- und Stahlbetonbau. 2013;108(11):783–91. <https://doi.org/10.1002/best.201300047>
- Scheerer S, Curbach M. Leicht Bauen mit Beton—Grundlagen für das Bauen der Zukunft mit bionischen und mathematischen Entwurfsprinzipien: Abschlussbericht SPP 1542 [Forschungsbericht]. Dresden: Scheerer and Curbach; 2022.
- Haist M, Bergmeister K, Curbach M, Forman P, Gaganelis G, Gerlach J, et al. Nachhaltig konstruieren und bauen mit Beton. In: Bergmeister K, Fingerloos F, Wörner J-D, editors. Beton-Kalender 2022. Berlin: Ernst & Sohn; 2022. p. 454–531.
- Kromoser B. Ressourceneffizientes Bauen mit Betonfertigteilen—Material—Struktur—Herstellung. In: Bergmeister K, Fingerloos F, Wörner J-D, editors. Beton-Kalender 2021. Berlin: Ernst & Sohn; 2021. p. 305–56.
- Stracke J, Kepplin R. Der BIM-Prozess in der Tragwerksplanung. Beton—und Stahlbetonbau. 2020;115(4):324–31. <https://doi.org/10.1002/best.201900097>
- Zimmert F, Braml T. Parametric modelling of free-form structural concrete beams and derivation of structural analysis models. Proceedings for the 6th fib International Congress 2022, Oslo, Norway: Novus Press; 2022. p. 1254–63.
- Zöller R, Ochlast A, Zimmert F, Braml T. Entwicklung von Prozessen zur automatisierten Planung und Herstellung von Stahlbetonbauteilen. Beton- und Stahlbetonbau. 2022;117(4):222–34. <https://doi.org/10.1002/best.202100102>
- Zimmert F, Braml T. Freiformbauteile im Stahlbeton-, Spannbeton- und Verbundbau: Berechnung von Querschnittswerten. Beton- und Stahlbetonbau. 2023;118(5):341–52. <https://doi.org/10.1002/best.202200110>
- Fleßner H. Ein Beitrag zur Ermittlung von Querschnittswerten mit Hilfe elektronischer Rechenanlagen. Der Bauingenieur. 1962;37(4):146–9.
- Lauer H. Der einachsige Spannungs- und Deformationszustand in beliebigen Stahlbetonquerschnitten bei räumlicher Beanspruchung unter Beachtung der Stoffgesetze nach DIN 1045 [Mitteilung]. Neubiberg: D. Könke; 1982.
- Marín J. Computing Unidimensional Normal Stress Resultants. J Struct Div. 1980;106(1):233–45. <https://doi.org/10.1061/JSDEAG.0005338>
- Witfeld H. Die Anwendung von Splines bei der Ermittlung von Querschnittswerten ebener Flächen. Ingenieur-Archiv. 1981;50:271–9.
- Niggel AK. Tragwerksanalyse am volumenorientierten Gesamtmodell—Ein Ansatz zur Verbesserung der computergestützten Zusammenarbeit im konstruktiven Ingenieurbau [Dissertation]. Technische Universität München. 2007.
- Koczyk S, Weese W. FEM-Lösung des Problems der St.-Venantschen Torsion mit Hilfe der Wölbfunktion. Technische Mechanik. 1991;12(2):125–30.
- Gruttmann F, Wagner W, Sauer R. Zur Berechnung von Wölbfunktion und Torsionskennwerten beliebiger Stabquerschnitte mit der Methode der finiten Elemente. Bauingenieur. 1998;73(3):138–43.
- Høgsberg J, Krenk S. Analysis of moderately thin-walled beam cross-sections by cubic isoparametric elements. Comput Struct. 2014;134:88–101. <https://doi.org/10.1016/j.compstruc.2014.01.002>
- Pilkey WD. Analysis and design of elastic beams—Computational methods. New York: Wiley; 2002.
- Sapountzakis EJ, Mokos VG. Warping shear stresses in nonuniform torsion of composite bars by BEM. Comput Methods Appl Mech Eng. 2003;192(39–40):4337–53. [https://doi.org/10.1016/S0045-7825\(03\)00417-1](https://doi.org/10.1016/S0045-7825(03)00417-1)
- Cottrell JA, Hughes TJR, Bazilevs Y. Isogeometric Analysis—Toward Integration of CAD and FEA. Chichester: John Wiley & Sons; 2009.
- Hughes TJR. The Finite Element Method—Linear Static and Dynamic Finite Element Analysis. New York: Dover Publications; 2000.
- Zilch K, Zehetmaier G. Bemessung im konstruktiven Betonbau—Nach DIN 1045-1 (Fassung 2008) und EN 1992-1-1 (Eurocode 2). 2nd ed. Berlin, Heidelberg: Springer Verlag; 2010.
- Stroud AH, Secrest D. Gaussian quadrature formulas. Englewood Cliffs: Prentice-Hall; 1966.
- Pilkey WD. Formulas for stress, strain, and structural matrices. 2nd ed. Hoboken: John Wiley & Sons; 2005.
- Muskhishvili NI. Some basic problems of the mathematical theory of elasticity—Fundamental equations, plane theory of elasticity, torsion and bending. 2nd ed. Leyden: Noordhoff; 1977.
- Rath DP, Ahlawat AS, Ramaswamy A. Shape Optimization of RC Flexural Members. J Struct Eng. 1999;125(12):1439–46. [https://doi.org/10.1061/\(ASCE\)0733-9445\(1999\)125:12\(1439\)](https://doi.org/10.1061/(ASCE)0733-9445(1999)125:12(1439))

## AUTHOR BIOGRAPHIES



**Florian Zimmert** earned his master's degree in civil engineering from the Technical University of Munich in 2015. After that he worked for several years in the field of structural design and conservation management of bridge structures in Germany. Florian Zimmert has been working as a research assistant at the University of the Bundeswehr Munich, Institute for Structural Engineering, since the end of 2018. His research topics address the geometric modeling and numerical calculation of free-form structures made of structural concrete. He is currently developing a software tool for the application of Isogeometric Analysis in this field. Furthermore, Florian Zimmert is involved with teaching in the field of bridge construction and prestressed concrete design. He also works as a freelance structural engineer.



**Thomas Braml** has held the professorship for structural concrete since April 2018. He worked for many years as a project engineer, project manager and later as a group leader in structural engineering in renowned engineering offices. Most recently, he worked as a managing partner in an engineering office for object and structural design and was responsible for the planning of numerous bridges as well as buildings and industrial structures

at home and abroad. His research focuses on protective structures, automation in construction and the implementation of digital twins for infrastructure structures. In his academic education, he holds a Dipl.-Ing. (FH) degree from the University of Applied Sciences in Deggendorf and a Dipl.-Ing. univ. degree from the Technical University of Dresden. Thomas Braml completed his PhD thesis in the field of reliability theory in structural concrete at the University of the Bundeswehr in Munich.

**How to cite this article:** Zimmert F, Braml T. Free-form reinforced concrete, prestressed concrete, and composite components: Calculation of cross-section values. *Civil Engineering Design*. 2024;5(5-6):95–106. <https://doi.org/10.1002/cend.202300010>